Identification of Serpin Determinants of Specificity and Selectivity for Furin Inhibition through Studies of α_1PDX (α_1-Protease Inhibitor Portland)-Serpin B8 and Furin Active-site Loop Chimeras*

Gonzalo Izaguirre, Lixin Qi, Mary Lima, and Steven T. Olson

From the Center for Molecular Biology of Oral Diseases and the Department of Periodontics, University of Illinois at Chicago, Chicago, Illinois 60612

*Running title: *Specificity determinants of the α_1PDX-furin reaction*

To whom correspondence should be addressed: Gonzalo Izaguirre, 801 South Paulina Street, MC 860, Chicago, IL 60612, Tel: 312-355-0573, Fax: 312-996-0943, e-mail: goniza@uic.edu

Keywords: serpin, furin, α_1PDX, serpin B8, proprotein convertase, serine protease, protease inhibitor

Background: α_1PDX and serpin B8 are proprotein convertase (PC) inhibitors whose specificity and selectivity for PCs are not understood.
Results: α_1PDX-serpin B8 and furin-PC chimeras revealed new serpin and protease (re)active-site and exosite determinants of reactivity.
Conclusion: α_1PDX reactive-site and exosite determinants may be exploited for engineering specificity and selectivity for inhibiting PCs.
Significance: Specific PC inhibitors will advance understanding of PC function and therapeutics.

SUMMARY

α_1PDX is an engineered serpin family inhibitor of the proprotein convertase (PC), furin, that exhibits high specificity but limited selectivity for inhibiting furin over other PC family proteases. Here, we characterize serpin B8, a natural inhibitor of furin, together with α_1PDX-serpin B8 and furin-PC chimeras to identify determinants of serpin specificity and selectivity for furin inhibition. Replacing reactive center loop (RCL) sequences of α_1PDX with those of serpin B8 demonstrated that both the P1-P4 RXXR recognition sequence as well as the P1'-P5' sequence are critical determinants of serpin specificity for furin. Alignments of PC catalytic domains revealed four variable active-site loops whose role in furin reactivity with serpin B8 was tested by engineering furin-PC loop chimeras. The furin 298-300 loop but not the other loops differentially affected furin reactivity with serpin B8 and α_1PDX in a manner that depended on the serpin RCL primed sequence. Modeling of the serpin B8-furin Michaelis complex identified serpin exosites in strand 3C close to the 298-300 loop whose substitution in α_1PDX differentially affected furin reactivity depending on the furin loop and serpin RCL primed sequences. These studies demonstrate that RCL primed residues, strand 3C exosites and the furin 298-300 loop are critical determinants of serpin reactivity with furin which may be exploited in the design of specific and selective α_1PDX inhibitors of PCs.

Furin is a member of the proprotein convertase (PC)[1] family of calcium-dependent serine proteases that have structural homology to subtilisin/kexin-type proteases and are characterized by their recognition of a distinctive P4Arg-X-Arg/Lys-P1Arg consensus cleavage site (1,2). PCs perform the intracellular and pericellular processing of a large number of peptide and protein precursors transiting the constitutive and regulated protein secretion pathways, including prohormones, growth factors and their receptors, matrix metalloproteases and integrins. PCs are thus pivotal in the control of cell signaling, proliferation, motility and adhesion (3,4). PC dysfunction is associated with a broad spectrum of diseases, including cancer, autoimmunity, and Alzheimer's. In addition, a number of significant human infectious organisms take advantage of host PC activity to promote their growth (5). PCs have been considered promising therapeutic drug targets, and the development of specific inhibitors is being intensely pursued (6,7). However, a limitation has been the lack of detailed

understanding of PC substrate specificity compounded by the similarity of PC catalytic domains (8,9). Moreover, most PC specificity studies have focused on the unprimed substrate binding pockets of the catalytic site and neglected the primed binding pockets (10).

Protein active-site directed inhibitors of PCs have been engineered by substituting the P4Arg-X-X-P1Arg sequence into the reactive sites of different families of protein protease inhibitors, including leech eglin-C (11), turkey ovomucoid (12), α_2-macroglobulin (13), and the serpin α_1-protease inhibitor or α_1PDX (14). However, the engineered PC target sequence is recognized by all PC family members and therefore such inhibitors are of limited use as therapeutics or research tools. Of particular note, protein protease inhibitors of the serpin family have been reported to be natural inhibitors of PCs, although their physiologic targets have not been defined (15-18). Serpins inhibit their target proteases by a distinctive suicide substrate mechanism that leads to the formation of a stable serpin-proteinase covalent inhibitory complex (19,20). Unlike most other protein protease inhibitor families, the specificity and selectivity of serpins for inhibiting their target proteases is achieved through recognition determinants in an exposed reactive center loop as well as in exosites surrounding this loop (20). Serpin B8 (also known as proteinase inhibitor 8, or PI8) is an intracellular serpin that was first shown to inhibit furin in vitro because of the presence in its RCL of two Arg-X-X-Arg sequences (15). It is the only human serpin that carries a PC recognition sequence in its RCL. Serpin B8 has been detected in a wide variety of human tissues (21) and been shown to inhibit furin in platelets (22). Similar natural serpin inhibitors of furin exist in insects and cephalochordates (16-18). An understanding of the determinants of specificity and selectivity of these natural serpins for their target PCs could therefore provide insights into the design of specific serpin inhibitors of PCs.

In the present study, we have sought to gain insights into designing specificity and selectivity in the engineered serpin inhibitor of furin, α_1PDX, by characterizing α_1PDX-serpin B8 chimeras as well as chimeras of furin in which variable active-site loops of the protease were replaced with those of other PCs. We demonstrate that in addition to the P4Arg-X-X-P1Arg recognition sequence in the serpin RCL, the primed RCL sequence plays a critical role in α_1PDX reactivity with furin and its ability to discriminate among different PC family members. Serpin exosites in strand 3 of β-sheet C are also shown to influence α_1PDX reactivity and selectivity for furin. The contribution of reactive site and exosite determinants of α_1PDX to reactivity with furin is further shown to be dependent on the furin 298-300 loop sequence. Our findings demonstrate the potential for engineering specific and selective α_1PDX inhibitors of furin and other PCs by targeting RCL and exosite determinants of this serpin.

EXPERIMENTAL PROCEDURES

Proteins–cDNA encoding serpin B8 was kindly provided by Dr. Walter Kisiel (University of New Mexico, Albuquerque, NM). Two stable monomeric forms of recombinant serpin B8 were engineered either by mutating the five surface cysteines at positions 5, 59, 340, 348 and 368 (as judged by molecular modeling) to serines (serpin B8-5S) or by mutating the five surface cysteines to serine and the five buried cysteines, residues 98, 108, 128, 317, and 368, to alanine (serpin B8-5S5A). Alanine rather than serine substitutions were found to be essential for expression of the latter variant. Wild-type and mutant forms of serpin B8 were expressed with a C-terminal His-tag in sf9 insect cells using the baculovirus expression system (Invitrogen). Cells were lysed by sonication after suspension in 20 mM Hepes buffer, pH 7.5, containing 50 mM NaCl, 20 mM imidazole, 6 mM $MgCl_2$, 1 mM $CaCl_2$, DNAse and protease inhibitor cocktail (Sigma). Serpin B8 was purified by first applying the cell lysate to a nickel affinity column (ProBond, Invitrogen) equilibrated in 20 mM Hepes, 100 mM NaCl, pH 7.5, washing with 5 volumes of 20 mM Hepes, 500 mM NaCl, pH 7.5 and then step-eluting the protein with equilibrating buffer containing 500 mM imidazole. Pooled and concentrated protein fractions were then applied to a Superdex 75 column (GE Healthcare) equilibrated and eluted in 20 mM Hepes, 100 mM NaCl, pH 7.5 buffer. Protein concentration was determined from the 280 nm absorbance using an extinction coefficient of 32,900 M^{-1} cm^{-1} calculated from the amino acid sequence (23). Both serpin B8 forms migrated on

SDS-PAGE as monomeric forms with the expected molecular weight under both nonreducing and reducing conditions, and proved to be very stable.

The full length furin cDNA was kindly provided by Dr. Gary Thomas (University of Pittsburgh, Pittsburgh, PA). Furin was expressed as a 53 kDa truncated form that included the first 579 residues up to the end of the P-domain, preceded by a FLAG sequence and followed by a C-terminal His-tag. Recombinant furin was produced as a secreted protein in Hi5 insect cells using the baculovirus expression system (Invitrogen). The culture media containing the expressed protein was first concentrated and buffer exchanged into 20 mM Hepes, 50 mM NaCl, 20 mM imidazole, 5 mM $CaCl_2$, 5 % glycerol, pH 7.5 by repeated ultrafiltration. Furin was purified by nickel affinity chromatography as with serpin B8 except that the exchange buffer was used for equilibration of the column. This was followed by gel filtration chromatography on Superdex 75 in the same equilibrating buffer without imidazole. Furin samples were supplemented with glycerol to 50 % prior to storage at -80^{o}C. Protein concentration was determined from the 280 nm absorbance using a calculated extinction coefficient of 87,820 M^{-1} cm^{-1} (23).

α_1PDX was engineered from an α_1PI C232S variant by changing both P1 Met and P4 Ala residues to Arg as in previous studies (14, 24). Wild-type and chimeric forms of α_1PDX were produced in *E. coli* BL21 cells using the T7 expression system (Invitrogen) and refolded from inclusion bodies as described (25). After refolding, α_1PDX was purified by ion exchange chromatography on DEAE-Sepharose at pH 6.5 followed by MonoQ (GE Healthcare) at pH 7.0, using linear sodium chloride gradients to elute the protein (24). Protein concentration was obtained from the 280 nm absorbance using an extinction coefficient of 27,000 M^{-1} cm^{-1} (26).

Mutagenesis of serpin B8, furin or α_1PDX cDNAs was done by PCR using specifically designed oligonucleotides from Integrated DNA Technologies and Pfu Turbo DNA polymerase from Stratagene according to the manufacturer's instructions. All mutations were confirmed by DNA sequencing. SDS-PAGE analysis indicated that all purifed wild-type and mutant recombinant proteins were routinely >95 % pure.

Furin Activity Assay- Furin activity was assayed by monitoring the linear rate of cleavage of the fluorogenic substrates, boc-Arg-Val-Arg-Arg-7-amido-methylcoumarin or pyr-Arg-Thr-Lys-Arg-amido-methylcoumarin (Bachem) at 100 μM, in 100 mM Hepes buffer, pH 7.5, containing 1 mM $CaCl_2$, 1 mM β-mercaptoethanol, 0.5 % Triton-X100, 0.1 % polyethylene glycol 8000 at 25 ^{o}C. Excitation and emission wavelengths were 380 and 460 nm, respectively. Michaelis-Menten parameters were determined from the dependence of initial rates of substrate cleavage on substrate concentration in the range 0.15-10 x K_M.

Furin Active-Site Titration-Fixed concentrations of wild-type or variant furins (100 nM) were incubated overnight at 25 ^{o}C with increasing concentrations of dec-Arg-Val-Lys-Arg-chloromethylketone (Bachem) in furin assay buffer adjusted to pH 5.5 to minimize hydrolysis of the chloromethylkeone inhibitor but allow complete inhibition of furin based on the measured k_{ass} for furin inhibition at this pH (~10^4 M^{-1} s^{-1}). Residual furin activity was then assayed and plotted as a function of the inhibitor concentration. Plots showed linear decreases in furin activity with endpoints of zero activity in all cases. The abscissa intercept of the linear regression fit of the data yielded the functional furin concentration. Furin and furin variants were found to be fully active.

Stoichiometry of serpin-furin reactions-The stoichiometry of inhibition for reactions of furin and furin variants with serpins was determined in furin assay buffer at 25 ^{o}C by incubating a fixed concentration of furin with increasing concentrations of serpin for a time allowing >95 % inhibition based on measured values of k_{ass}. Residual furin activity was assayed and plotted as a function of the molar ratio of serpin to protease. Linear regression fits yielded the stoichiometry of inhibition from the abscissa intercept.

Kinetics of furin inhibition by serpins-The kinetics of serpin B8 or α_1PDX inhibition of furin were studied in furin assay buffer at 25 ^{o}C by continuous or discontinuous assays of the loss of furin activity under pseudo-first order reaction conditions as in previous studies, with the serpin concentration at least ten-fold higher than the protease concentration (24). In the continuous assay, serpin inhibition of furin was monitored in

the presence of 100 μM furin fluorogenic substrate from the exponential decrease in the rate of cleavage of substrate as described for the furin activity assay. The rate of fluorescence increase due to furin cleavage of the substrate in the absence of inhibitor remained linear over the range of fluorescence amplitudes observed for furin inhibition reactions, indicating no significant substrate depletion. For reactions with $t_{1/2}$ >1 min, furin inhibition was followed by a discontinuous assay in which reactions were quenched at different reaction times by 10–fold dilution with substrate and the initial rate of substrate cleavage was measured as in the furin activity assay. Observed pseudo-first order rate constants (k_{obs}) were obtained by fitting progress curves of substrate hydrolysis in the continuous assay or the fractional loss in furin activity with time for the discontinuous assay by a single exponential equation. Apparent second order association rate constants were obtained from slopes of linear regression fits of the dependence of k_{obs} on the effective inhibitor concentration; i.e., after correcting for the competitive effect of substrate in the case of continuous assays by dividing by the factor, $1 + [S]_o / K_M$, where $[S]_o$ is the substrate concentration and K_M is the Michaelis constant for substrate hydrolysis. At least five different inhibitor concentrations ranging from 5-50 nM for the fastest reactions (second order rate constants of ~10^6 M^{-1} s^{-1}) or 200-800 nM for the slowest reactions (second order rate constants 10^3-10^4 M^{-1} s^{-1}) were employed. To correct for the fraction of serpin that is cleaved by furin along a competing substrate pathway, the apparent association rate constant was multiplied by the stoichiometry of inhibition to yield k_{ass}, the association rate constant for reaction along the inhibitory pathway.

SDS-PAGE-The purity of recombinant proteins and the ability of serpins to form SDS-stable complexes with proteases were analyzed by SDS-PAGE under non-reducing conditions using the Laemmli buffer system (27).

Protein Structure Modeling-Models of the serpin B8 structure were obtained using the SWISS-MODEL tool for protein homology modeling. The serpin B8 amino acid sequence was threaded using as templates the x-ray crystal structures of the serpins, maspin (PDB, entry 1XQJ), antithrombin (PDB, entry 1EO3) and $\alpha_1$antitrypsin (PDB, entry 1ATU). Modeling of the serpin B8-furin Michaelis complex was done using the program DeepView (Swiss PDB-Viewer). The serpin B8 model and the X-ray structure of the furin catalytic domain (PDB, entry 1P8J) were superimposed on the Michaelis complex structures of antithrombin-factor Xa, (PDB, entry 2GD4) antithrombin-thrombin (PDB, entry 1SR5), and α_1PI-trypsin (PDB, entry 1OPH). To superimpose the subtilisin-type fold of furin on the chymotrypsin family protease components of the Michaelis complexes, the structurally conserved catalytic triads were aligned.

RESULTS

Characterization of the serpin B8-furin reaction-To provide insights into engineering a specific and selective serpin inhibitor of PCs, we first characterized serpin B8, a natural intracellular inhibitor of furin. The propensity of wild-type serpin B8 to form disulfide-linked multimers through its ten cysteine residues prompted us to engineer stable monomeric forms of the serpin by mutating the cysteines to serine or alanine (see Experimental Procedures). The ability of the two stable serpin B8 variants to inhibit furin was assessed by continuous monitoring of the kinetics of furin cleavage of a reporter fluorogenic substrate under pseudo-first order conditions. Reactions performed at increasing serpin B8 concentrations produced a family of inhibition progress curves that were characterized by increasing rates of furin inhibition and decreasing fluorescence amplitudes (fig. 1). Observed pseudo-first order rate constants (k_{obs}) derived from the progress curves showed a proportional dependence on serpin B8 concentration for both serpin B8 variants (fig. 1), yielding similar apparent second order rate constants of ~10^5 M^{-1} s^{-1} for inhibition of furin. Stoichiometries of inhibition (SI), assessed from titrations of the loss in furin activity as a function of increasing molar ratios of serpin B8 to furin, yielded values of 1.5 and 2.2 moles inhibitor/mole protease for serpin B8-5S and serpin B8-5S5A, respectively (fig. 1). The observation of stoichiometries greater than 1 suggested that a fraction of the serpin was being cleaved by furin as a substrate, in accordance with the branched pathway suicide substrate mechanism by which serpins inhibit proteases (19). This was verified by SDS-PAGE analysis of the products of the reaction which showed both

serpin-protease complex and cleaved serpin products (fig. 2). Correction of apparent second rate constants for the different extents of substrate reaction by multiplying by the SI yielded similar association rate constants for reaction along the inhibitory pathway (k_{ass}) of ~2 x 10^5 M^{-1} s^{-1} for the two serpin B8 variants that were in reasonable agreement with reported values for wild-type serpin B8 (15).

Two Arg-X-X-Arg substrate recognition sequences for PCs exist in the reactive center loop (RCL) of serpin B8, one that aligns with the P4-P1 sequence and the other with the P1-P3' sequence of other serpins (fig. 2). To confirm that the former is the functional site for inhibition of furin and determine whether the latter might be an alternate site of cleavage, single alanine mutations of the arginine residues 336, 339 and 342 were introduced in serpin B8-5S to eliminate one or both target sequences. Of the three variants tested, only the R342A variant that retained the P4Arg336-P1Arg339 sequence was a functional inhibitor of furin (fig. 2), confirming the importance of the furin recognition sequence in the P4-P1 positions for inhibitor function. Surprisingly, the R336A variant containing the alternative P1Arg339-P3'Arg342 furin recognition sequence was completely unreactive as an inhibitor or substrate of furin. This suggested that the cleaved serpin B8 produced in the reaction of the parent serpin B8-5S with furin does not derive from an alternative cleavage after Arg342, but rather arises from cleavage after P1Arg339. Interestingly, the R342A variant differed from the parent serpin B8-5S in producing only inhibitory complexes with no cleaved serpin (fig. 2) and inhibiting furin with a 3-fold lower k_{ass} (table 1). This indicated that the P3' Arg342 is an important determinant of serpin B8 reactivity with furin both as an inhibitor and a substrate.

RCL determinants of serpin specificity for furin- We next investigated whether we could transfer the determinants of serpin B8 specificity for furin to α_1PDX, an engineered inhibitor of furin derived from the extracellular serpin, α_1PI, by replacing the P4 and P1 RCL residues with Arg to generate the RXXR recognition sequence of PCs (14). α_1PDX inhibited furin with a k_{ass} of 1 x 10^6 M^{-1} s^{-1} and a stoichiometry of inhibition of 1, in good agreement with previous studies (28) (table 1). α_1PDX is thus a ~5-fold faster inhibitor of furin than serpin B8. To determine whether this difference in specificity for furin was encoded in the RCL sequence, we characterized α_1PDX-serpin B8 chimeras in which the unprimed (P6-P1), the primed (P1'-P5') or the full (P6-P5') RCL sequences of α_1PDX were replaced with those of serpin B8 (fig. 3). Replacing just the P6-P1 RCL sequence of α_1PDX increased k_{ass} for furin inhibition 2-fold over that of α_1PDX. By contrast, replacing the primed P1'-P5' or full P6-P5' RCL sequences of α_1PDX with that of serpin B8 decreased k_{ass} for furin inhibition 20-fold and 10-fold, respectively, from that of α_1PDX (fig. 3 and table 1). The inhibition stoichiometries were not significantly affected by these RCL changes. These findings suggested that the unprimed RCL sequence of serpin B8 confers a modestly greater reactivity and the primed RCL sequence a substantially lower reactivity for furin than the corresponding sequences of α_1PDX.

Surface loops in the furin catalytic domain affect serpin reactivity- To assess whether furin determinants exist to regulate the specificity and selectivity of serpin B8 for furin and other PCs, we examined sequence alignments of the catalytic domains of seven human PCs. The alignments revealed a high degree of sequence conservation as previously noted (10), except for four surface loops surrounding the active-site which showed high sequence variability. These loops comprise residues 187-189, 298-300, 345-350, and 357-359 (figs. 4 & 5). To determine whether these loops contributed to the high reactivity of furin with serpin B8, we expressed four furin variants in which the residues of each variable loop were all mutated to Ala. The effect of the loop mutations on furin catalytic activity was first tested by studying the kinetics of cleavage of two synthetic RXXR fluorogenic substrates. The four loop mutants each showed decreases in the overall specificity constants i.e., k_{cat}/K_M, for hydrolysis of the two substrates ranging from 1.1-1.2-fold for the 345-350 loop mutant to 6-8-fold for the 187-189 loop mutant (fig. 6). These decreases resulted mostly from changes in k_{cat} (table 2).

The effect of the loop mutations on the kinetics and stoichiometry of furin inhibition by serpin B8 and α_1PDX was next determined. Mutations of three of the furin loops, 187-189, 345-350 and

357-359, resulted in decreases in k_{ass} for reaction of furin with the two serpins that differed by at most ~2-fold from the decreases observed in k_{cat}/K_M for substrate hydrolysis, i.e., 1.6-4-fold (fig. 6 and table 3). By contrast, the 298-300 loop mutant affected furin reactivity with the two serpins quite differently. k_{ass} for reaction with serpin B8 was thus decreased 4-fold, whereas k_{ass} for reaction with α_1PDX was *increased* ~2-fold relative to wild-type furin, both in contrast to the ~2-fold reduction in k_{cat}/K_M for hydrolysis of the RXXR substrate. This suggested that the furin 298-300 loop differentially affects reactivity with the two serpins through determinants that do not involve the RCL RXXR recognition sequence.

To assess whether the serpin determinants that mediate this differential reactivity with furin reside in the RCL, we compared the reactivity profiles of the furin loop mutants with α_1PDX and the α_1PDX-serpin B8 RCL chimeras (fig. 6 and table 3). Swapping the full serpin B8 RCL into α_1PDX dramatically altered α_1PDX reactivity with the furin 298-300 loop mutant, but minimally affected reactivity with the other furin loop mutants. k_{ass} for the α_1PDX RCL chimera-furin reaction was thus decreased 4-fold by the furin loop mutation, in marked contrast to the increase in k_{ass} observed for the α_1PDX-furin reaction but similar to the decrease in k_{ass} observed for the serpin B8-furin reaction. Significantly, replacing just the P1'-P5' residues of α_1PDX with those of serpin B8 resulted in a change in k_{ass} for inhibition the furin 298-300 loop mutant relative to furin like that of the full RCL swap whereas replacing just the P1-P6 α_1PDX residues with those of serpin B8 resulted in no change in k_{ass} for mutant and wild-type furin reactions. These findings suggested that the furin 298-300 loop affects α_1PDX reactivity largely through interactions with the primed side of the RCL.

PC variability of the 298-300 loop influences serpin reactivity- The observation that replacing the furin 298-300 loop sequence but not the other furin variable loops with alanines produced a large *differential* reactivity of furin with serpin B8 and α_1PDX, suggested that the 298-300 loop might encode specificity determinants that govern PC reactivity with serpins. In order to test this possibility, we constructed a panel of furin-PC chimeras in which the amino acid sequence of the furin 298-300 loop was substituted with the homologous sequences from other PCs (fig. 7 & table 4). The kinetic parameters for the reaction of the chimeras with one fluorogenic substrate showed alterations in k_{cat}/K_M that varied from 3-fold lower to 1.3-fold higher than wild-type furin. These variations mostly reflected differences in k_{cat}.

Notably, the furin 298-300 loop chimeras showed significantly greater reductions in reactivity with serpin B8 than with the synthetic substrate (fig. 7 and table 5) but showed either minimal change or up to 2.4-fold enhancements in reactivity with α_1PDX relative to wild-type furin. Again, substituting the serpin B8 P6-P5' residues into α_1PDX switched the reactivity profile with the furin chimeras to resemble that of serpin B8. As a result, the reactivities of each furin 298-300 loop chimera exhibited marked differences of 10-95-fold between α_1PDX and the α_1PDX-serpin B8 RCL chimera. Such findings supported the idea that the 298-300 loop sequence was an important determinant of the differential reactivities of furin with α_1PDX and serpin B8.

Strand 3C residues influence α_1PDX *reactivity with furin*- Since our data suggested that the 298-300 loop of furin affects serpin reactivity through interactions with the RCL primed sequence, we investigated whether this loop might also affect serpin reactivity through interactions with exosites outside the RCL. To localize such exosites, we constructed a molecular model of the serpin B8-furin Michaelis complex using the x-ray crystal structure of the furin catalytic domain together with the structures of several serpin-protease Michaelis complexes as a template (fig. 8). Placement of the subtilisin family protease, furin, in the Michaelis complexes with chymotrypsin family proteases was based on the common catalytic triad structures of subtilisin and chymotrypsin family proteases. The furin 298-300 loop was observed to closely approach residues Phe198 and Glu 200 in strand 3 of β-sheet C of serpin B8 in all models.

To determine whether these strand 3C residues influenced serpin reactivity with furin, the homologous strand 3C residues in α_1PDX, Lys222 and Leu224, were mutated to the serpin B8-like residues, Tyr and Glu, respectively. k_{ass} for reaction of furin with the α_1PDX-YE s3C chimera

was reduced by 5-fold and the inhibition stoichiometry was modestly increased relative to that with α_1PDX (table 1), indicating a marked effect on reactivity comparable to that of the serpin B8 RCL swap. To determine whether this change in reactivity resulted from interactions with the furin 298-300 loop, we measured k_{ass} and SI for reaction of the α_1PDX-YE chimera with the four furin loop mutants (fig. 9 and table 3). The reactivity of α_1PDX-YE with the furin loop variants was reduced in all cases from that of wild-type furin, similar to the reactivity changes of α_1PDX with the furin variants except for the 298-300 loop variant. Whereas α_1PDX-YE showed a 2-fold lower reactivity with the furin 298-300 loop mutant, α_1PDX exhibited a 2-fold higher reactivity with the variant than furin (figs. 6 & 9).

To further probe whether the effects of the α_1PDX strand 3C mutations on furin reactivity depended on the furin 298-300 loop sequence, we measured k_{ass} and SI for the reactions of α_1PDX-YE with the panel of furin 298-300 loop mutants (fig. 9 and table 5). The reactivity profile of α_1PDX-YE with the furin loop chimeras showed marked differences from that of α_1PDX in the case of the PC1 and PC5 loop chimeras. These chimeras thus showed reactivity enhancements with α_1PDX-YE relative to wild-type furin that were much greater (4.4-4.5-fold) than those observed with α_1PDX (2-fold) (fig. 7). Overall, the effects of the strand 3C mutations on α_1PDX reactivity with each of the furin 298-300 loop variants varied over a wide range from 2.3-fold for the PC5 loop variant to 12-fold for the triple alanine variant, indicating a significant dependence of the reactivity changes on the 298-300 loop sequence.

Synergistic effects of RCL and strand 3C determinants on α_1PDX *reactivity with furin*- We next investigated the effects of combining the RCL and strand 3C mutations in α_1PDX on furin reactivity (fig. 9 and table 5). The α_1PDX-serpin B8 P6-P5'-YE variant exhibited a striking ~730-fold loss in reactivity relative to α_1PDX. This reactivity loss was notable in that it greatly exceeded the additive losses of the RCL and strand 3C mutations alone (i.e., 10-fold and 5-fold, respectively) (fig. 10). The low reactivity of the α_1PDX dual RCL/strand 3C chimera with furin was further reduced with all furin alanine loop variants except for the 298-300 loop variant (fig. 9 & table 5). Again, the α_1PDX reactivity losses with each of the furin variants was greater than the additive losses expected from the individual mutations alone except for the 298-300 loop variant whose reactivity loss was additive (fig. 10). Remarkably, the reactivity profile of the α_1PDX dual RCL/strand 3C chimera with the panel of 298-300 furin loop chimeras differed substantially from that of α_1PDX, the single RCL or strand 3C α_1PDX chimeras or the RXXR substrate (fig. 9 & table 5). The furin chimeras thus showed the most marked alterations in furin reactivity with the α_1PDX dual chimera that ranged from ~2-fold lower (PC2 and PACE4) to 17-fold higher (PC5) than furin. As a result, α_1PDX reactivity losses with each of the furin 298-300 loop chimeras caused by the dual RCL and strand 3C mutations varied dramatically from ~100-1600-fold, indicating a major dependence of the reactivity loss on the furin 298-300 loop sequence (fig. 10).

DISCUSSION

Furin and other members of the PC family of proteases play critical roles in the processing of a variety of proteins to their biologically active form (3-5). Since PCs have been implicated in the pathogenesis of numerous diseases, specific inhibitors of these enzymes could be of great potential value as research tools and therapeutics (6,7). α_1PDX was engineered to be a furin inhibitor by replacing the P1 and P4 RCL residues of α_1PI with Arg, but the recognition of the consensus RXXR sequence by all PC family members makes this inhibitor unsuitable for selective targeting of individual PCs (14).

Our studies used a chimeric approach to investigate whether the natural PC inhibitor, serpin B8, possessed determinants that could transform α_1PDX into a specific and selective inhibitor of PCs. Stable recombinant forms of serpin B8 were shown to inhibit furin at a physiologically significant rate through the P1-P4 RXXR recognition sequence, in agreement with previous reports (15) and the observation that serpin B8-furin complexes are detectable in platelets (22). A second RXXR sequence in the P1-P3' RCL residues of serpin B8 was found to be unreactive with furin, although the P3' Arg in this sequence

contributed 3-fold to the specificity of serpin B8 for inhibiting furin.

α_1PDX was surprisingly found to be a 5-fold faster inhibitor of furin than serpin B8. This difference in specificity was largely accounted for by the different RCL sequences of the two serpins. Whereas the P1-P6 sequence of serpin B8 enhanced α_1PDX specificity for furin by 2-fold, the serpin B8 P1'-P5' sequence reduced α_1PDX specificity for furin by 20-fold. Substituting the full P6-P5' serpin B8 sequence into α_1PDX produced an additive net 10-fold reduction in specificity for furin, within 2-fold of that of serpin B8. These findings demonstrate a major impact of the primed RCL sequence on serpin reactivity with furin in addition to the established importance of the unprimed RXXR sequence. The primed sequence thus represents an important overlooked determinant for engineering specificity and selectivity in α_1PDX for PC family members.

The determinants of serpin reactivity with furin were additionally probed in the protease. Four variable loops surrounding the active-site were identified by sequence alignments of PC catalytic domains. All alanine mutations of these loops resulted in moderate reductions in k_{cat}/K_M for furin cleavage of RXXR peptide substrates and comparable reductions in k_{ass} for furin inhibition by serpin B8 and α_1PDX except for the 298-300 loop mutations which showed markedly different effects on k_{ass} for the two serpins. Mutations in this loop thus enhanced reactivity with α_1PDX and depressed reactivity with serpin B8. Substituting the primed or full serpin B8 RCL but not the unprimed RCL sequence into α_1PDX reversed the effect of the 298-300 loop mutation on furin reactivity to that observed with serpin B8. These findings suggest that interactions of the furin 298-300 loop with the primed RCL sequence of serpin B8 contribute positively to reactivity whereas interactions of the furin loop with the primed sequence of α_1PDX antagonize reactivity. The importance of furin 298-300 loop interactions with RCL primed residues in determining reactivity is in keeping with this loop residing close to the primed substrate binding pockets of the protease (29).

Further substitutions of the 298-300 loops of other PCs into furin similarly revealed effects on α_1PDX reactivity that differed significantly from the effects on serpin B8 reactivity or RXXR peptide substrate reactivity. Again, substituting the serpin B8 RCL into α_1PDX altered the effects of the 298-300 loop variants on α_1PDX reactivity to resemble more closely those on serpin B8. The 298-300 loop sequences of PCs thus contribute to variable reactivities with serpin B8 and α_1PDX through differential interactions with the primed RCL sequence. Such differential interactions may contribute to the selectivity of serpin B8 for different PCs and could be exploited for engineering selective PC inhibitors.

Alanine mutations of the three other furin loops also exhibited small differential effects on serpin B8 and α_1PDX reactivity, but these effects were marginally different from the changes in RXXR substrate reactivity. These loops thus appear to mostly affect furin active-site interactions with the serpin P1-P4 RXXR recognition sequence Nevertheless, the loops make important contributions to furin reactivity with serpins, the 187-189 loop being of particular importance given the significant negative effects of mutating this loop on furin reactivity. The variable sequences of these loops in PC family members suggests that they could contribute to variable reactivities of serpin B8 with PCs and that such variability might be exploited in engineering selectivity in α_1PDX for different PCs.

Our finding that the furin 298-300 loop influences reactivity with serpins lead us to explore potential interactions of this loop with exosites on the serpin body. A model of the serpin B8-furin Michaelis complex revealed strand 3C residues of serpin B8 that were close to this loop. Substitution of serpin B8-like strand 3C residues into the homologous residues of α_1PDX resulted in a loss of furin reactivity comparable to that caused by substituting the serpin B8 RCL into α_1PDX. This reactivity loss appeared to involve the furin 298-300 loop sequence since substituting the sequences of other PC loops showed that the reactivity losses of the α_1PDX-serpin B8 strand 3C chimera strongly depended on the furin loop sequence. The strand 3C exosites thus appear to perturb furin 298-300 loop interactions with the α_1PDX primed RCL sequence that govern reactivity.

Combining the serpin B8 strand 3C substitutions with the serpin B8 RCL substitution

in α_1PDX resulted in an unexpectedly dramatic ~700-fold loss in furin reactivity, i.e., greater than the loss expected from additive effects of the mutations. Notably, the four furin alanine loop mutants showed similar large losses in reactivity with the dual chimera that reflected synergistic effects of the individual serpin B8 substitutions in the chimera except for the 298-300 loop mutant whose reactivity losses reflected additive effects of the individual substitutions. This suggested that interactions among the furin 298-300 loop, the serpin primed RCL sequence, and the strand 3C exosite are strongly coupled and that this coupling is lost by mutating the furin loop to alanines (30, 31). This conclusion is supported by the finding that the extent of coupling was dependent on the furin 298-300 loop sequence with the wild-type sequence showing the largest coupling and the PC5 sequence showing no coupling. Notably, such differential coupling effects significantly enhanced the selectivity of the α_1PDX dual chimera for the furin 298-300 loop mutants. The observation that the reactivity of the dual chimera with furin is comparable in order of magnitude to the k_{cat}/K_M values for RXXR substrate cleavage suggests that the reactivity of this variant with furin may be governed solely by the RXXR sequence in the serpin RCL (32). This could result from the strand 3C mutations abrogating the contribution of the primed RCL sequence to reactivity. However, such an abrogation must be specific to the α_1PDX dual chimera since serpin B8 possesses the RCL and similar strand 3C determinants of this chimera but shows a ~100-fold higher reactivity. The effects of the strand 3C exosite residues on serpin reactivity thus appear to markedly depend on their context in the two serpins with the negative effects of the exosite residues expressed only in α_1PDX. Importantly, our findings demonstrate that serpin exosites can have a profound effect on furin reactivity as a result of their perturbing protease active-site interactions with the serpin RCL and these perturbing effects can be exploited to engineer specificity and selectivity for inhibiting PCs. Together, our findings suggest the potential for engineering specific and selective serpin inhibitors of PCs utilizing α_1PDX as a scaffold by targeting RCL and exosite determinants of α_1PDX that affect PC specificity.

REFERENCES

1. Molloy, S.S., Bresnahan, P.A., Leppla, S.H., Klimpel, K.R., and Thomas, G. (1992) Human furin is a calcium-dependent serine endoprotease that recognizes the sequence Arg-X-X-Arg and efficiently cleaves anthrax toxin protective antigen. *J. Biol. Chem.* **267**, 16396-16402
2. Walker, J.A., Molloy, S.S., Thomas, G., Sakaguchi, T., Yoshida, T., Chambers, T.M., and Kawaoka, Y. (1994) Sequence specificity of furin, a proprotein-processing endoprotease, for the hemagglutinin of a virulent avian influenza virus. *J. Virol.* **68,** 1213-1218
3. Scamuffa, N., Calvo, F., Chretien, M., Seidah, N.G., and Khatib, A.M. (2006) Proprotein convertases: lessons from knockouts. *FASEB J.* **20,** 1954-1963
4. Seidah, N.G., Mayer, G., Zaid, A., Rousselet, E., Nassoury, N., Poirier, S., Essalmani, R., and Prat, A. (2008) The activation and physiological functions of the proprotein convertases. *Int. J. Biochem.Cell Biol.* **40,** 1111-1125
5. Artenstein, A.W., and Opal, S.M. (2011) Proprotein convertases in health and disease. *N. Engl. J. Med.* **365,** 2507-2518
6. Seidah, N.G., and Prat, A. (2012) The biology and therapeutic targeting of the proprotein convertases. *Nat. Rev. Drug Discov.* **11,** 367-383
7. Couture, F., D'Anjou, F., and Day, R. (2011) On the cutting edge of proprotein convertase pharmacology: from molecular concepts to clinical applications. *Biomol. Concepts.* **2,** 421-438
8. Fugere, M., and Day, R. (2002) Inhibitors of the subtilase-like pro-protein convertases (SPCs). *Curr.Pharm.Des.* **8,** 549-562
9. Basak, A. (2005) Inhibitors of proprotein convertases. *J. Mol. Med. (Berl).* **83,** 844-855
10. Henrich, S., Lindberg, I., Bode, W., and Than, M.E. (2005) Proprotein convertase models based on the crystal structures of furin and kexin: explanation of their specificity. *J. Mol. Biol.* **345,** 211-227

11. Komiyama, T., and Fuller, R.S. (2000) Engineered eglin c variants inhibit yeast and human proprotein processing proteases, Kex2 and furin. *Biochemistry.* **39,** 15156-15165
12. Lu, W., Zhang, W., Molloy, S.S., Thomas, G., Ryan, K., Chiang, Y., Anderson, S., and Laskowski, M.,Jr (1993) Arg15-Lys17-Arg18 turkey ovomucoid third domain inhibits human furin. *J. Biol. Chem.* **268,** 14583-14585
13. Van Rompaey, L., Ayoubi, T., Van De Ven, W., and Marynen, P. (1997) Inhibition of intracellular proteolytic processing of soluble proproteins by an engineered alpha 2-macroglobulin containing a furin recognition sequence in the bait region. *Biochem. J.* **326 (Pt 2),** 507-514
14. Anderson, E.D., Thomas, L., Hayflick, J.S., and Thomas, G. (1993) Inhibition of HIV-1 gp160-dependent membrane fusion by a furin-directed alpha 1-antitrypsin variant. *J. Biol. Chem.* **268,** 24887-24891
15. Dahlen, J.R., Jean, F., Thomas, G., Foster, D.C., and Kisiel, W. (1998) Inhibition of soluble recombinant furin by human proteinase inhibitor 8. *J. Biol. Chem.* **273,** 1851-1854
16. Osterwalder, T., Kuhnen, A., Leiserson, W.M., Kim, Y.S., and Keshishian, H. (2004) Drosophila serpin 4 functions as a neuroserpin-like inhibitor of subtilisin-like proprotein convertases. *J. Neurosci.* **24,** 5482-5491
17. Richer, M.J., Keays, C.A., Waterhouse, J., Minhas, J., Hashimoto, C., and Jean, F. (2004) The Spn4 gene of Drosophila encodes a potent furin-directed secretory pathway serpin. *Proc. Natl. Acad. Sci. U.S.A.* **101,** 10560-10565
18. Bentele, C., Kruger, O., Todtmann, U., Oley, M., and Ragg, H. (2006) A proprotein convertase-inhibiting serpin with an endoplasmic reticulum targeting signal from Branchiostoma lanceolatum, a close relative of vertebrates. *Biochem. J.* **395,** 449-456
19. Silverman, G.A., Bird, P.I., Carrell, R.W., Church, F.C., Coughlin, P.B., Gettins, P.G., Irving, J.A., Lomas, D.A., Luke, C.J., Moyer, R.W., Pemberton, P.A., Remold-O'Donnell, E., Salvesen, G.S., Travis, J., and Whisstock, J.C. (2001) The serpins are an expanding superfamily of structurally similar but functionally diverse proteins. Evolution, mechanism of inhibition, novel functions, and a revised nomenclature. *J. Biol. Chem.* **276,** 33293-33296
20. Gettins, P.G., and Olson, S.T. (2009) Exosite determinants of serpin specificity. *J. Biol. Chem.* **284,** 20441-20445
21. Strik, M.C., Bladergroen, B.A., Wouters, D., Kisiel, W., Hooijberg, J.H., Verlaan, A.R., Hordijk, P.L., Schneider, P., Hack, C.E., and Kummer, J.A. (2002) Distribution of the human intracellular serpin protease inhibitor 8 in human tissues. *J. Histochem. Cytochem.* **50,** 1443-1454
22. Leblond, J., Laprise, M.H., Gaudreau, S., Grondin, F., Kisiel, W., and Dubois, C.M. (2006) The serpin proteinase inhibitor 8: an endogenous furin inhibitor released from human platelets. *Thromb. Haemost.* **95,** 243-252
23. Gill, S.C., and von Hippel, P.H. (1989) Calculation of protein extinction coefficients from amino acid sequence data. *Anal. Biochem.* **182,** 319-326
24. Izaguirre, G., Rezaie, A. R., and Olson, S. T. (2009) Engineering functional antithrombin exosites in α_1-proteinase inhibitor that specifically promote the inhibition of factor Xa and factor IXa. *J. Biol. Chem.* **284**, 1550-1558
25. Kwon, K.S., Lee, S., and Yu, M.H. (1995) Refolding of alpha 1-antitrypsin expressed as inclusion bodies in Escherichia coli: characterization of aggregation. *Biochim. Biophys. Acta.* **1247,** 179-184
26. Pannell, R., Johnson, D., and Travis, J. (1974) Isolation and properties of human plasma alpha-1-proteinase inhibitor. *Biochemistry.* **13,** 5439-5445
27. Laemmli, U. K. (1970) Cleavage of structural proteins during the assembly of the head of bacteriophage T4. *Nature* **227**, 680-685
28. Dufour, E. K., Denault, J.-B., Hopkins, P. C. R. and Leduc, R. (1998) Serpin-like properties of a1-antitrypsin Portland towards furin convertase. *FEBS Lett.* **426**, 41-46
29. Henrich, S., Cameron, A., Bourenkov, G. P., Kiefersauer, R., Huber, R., Lindberg, I., Bode, W., and Than, M. E. (2003) The crystal structure of the proprotein processing furin explains its stringent specificity. *Nat. Struc. Biol.* **10**, 520-526

30. Horovitz, A. (1987) Non-additivity in protein-protein interactions. *J. Mol. Biol*. **196**, 733-735
31. Di Cera, E. (1998) Site-specific thermodynamics: understanding cooperativity in molecular recognition. *Chem. Rev*. **98**, 1563-1591
32. Dementiev, A., Simonovic, M., Volz, K., and Gettins, P. G. W. (2003) Canonical inhibitor-like interactions explain reactivity of α_1-proteinase inhibitor Pittsburgh and antithrombin with proteinases. *J. Biol. Chem.* **278**, 37881-37887

Acknowledgements- We thank Saivenkat Vagvala and Danté Brown for excellent technical assistance with the studies and Dr. Peter Gettins of the UIC Department of Biochemistry and Molecular Biology for his critical comments on the manuscript.

FOOTNOTES

* This work was supported by NIH grant R37-HL39888
1 Abbreviations used are: PC, proprotein convertase; α_1PI, α_1-protease inhibitor; α_1PDX, α_1-protease inhibitor Portland variant with P1 and P4 residues replaced with Arg; RCL, reactive center loop

FIGURE LEGENDS

Fig. 1 **Kinetics and stoichiometry of serpin B8 inhibition of furin** A, Progress curves for inhibition of 2.6 nM furin by increasing concentrations of serpin B8-5S monitored from the exponential decrease in rate of furin cleavage of fluorogenic substrate as a function of time. B, Dependence of observed pseudo-first order rate constants (k_{obs}) derived from exponential fits of progress curves in panel A on the serpin B8 concentration corrected for fluorogenic substrate competition as described in Experimental Procedures. Data is shown for reactions of serpin B8-5S (●) and serpin B8-5S5A (○). The slope of linear regression fits of the data (solid lines) provided the apparent second order association rate constants ($k_{ass,app}$) for the inhibition reaction. C, Stoichiometric titrations of furin with serpin B8 analyzed from the furin activity remaining after complete reaction with increasing molar ratios of serpin B8 to furin. Shown are reactions with serpin B8-5S (●) and serpin B8-5S5A (○). The stoichiometry of inhibition (SI) was obtained from the abscissa intercept of linear regression fits of titrations (solid lines).

Fig. 2 **SDS-PAGE analysis of reactions of parent and RCL variant forms of serpin B8-5S with furin** A, Sequence of the reactive center loop P6-P5' region of serpin B8-5S showing the two RXXR sequences at P4-P1 and P1-P3'. B SDS-PAGE analysis of the reactions of parent and three single Arg→Ala variant forms of serpin B8-5S (4 μg) with furin (1 μg) as indicated. Protein bands were stained with Coomassie Blue. Labels on the right indicate the position of serpin-protease complex and cleaved serpin bands. Molecular weight standards are in the leftmost lane.

Fig. 3 **Comparison of the reactivities of serpin B8, α_1PDX and α_1PDX-serpin B8 RCL chimeras with furin** A, RCL sequences of α_1PDX and α_1PDX-serpin B8 chimeras in which α_1PDX P6-P1, P1'-P5' and P6-P5' residues were replaced with those of serpin B8. B, Bar graph comparing k_{ass} for the reactions of serpin B8-5S, α_1PDX and the three α_1PDX-serpin B8 chimeras with furin from table 1. Values at the top of bars are k_{ass} expressed relative to that for the serpin B8 reaction.

Fig. 4. **Sequence alignments of PC catalytic domains** Sequence alignments of the catalytic domains of seven human PC family members with black, gray and white coloring reflecting high conservation, moderate conservation and poor conservation of individual residues, respectively. The inverted triangles indicate the catalytic triad residues. The indicated four surface loops surrounding the enzyme active site, comprising residues 187-189, 298-300, 345-350, and 357-359, show high sequence variability.

Fig. 5 **Location of furin variable surface loops in the furin catalytic domain-** The murine furin catalytic domain structure (PDB 1P8J) depicted in ribbons showing the four variable loops surrounding the catalytic cleft in stick representation: loop 187-189 (yellow), loop 298-300 (green), loop 345-350 (cyan), and loop 357-359 (purple). The catalytic triad residues are shown in stick (red). The 298-300 loop lies adjacent to the S2' binding pocket (29). The figure was prepared using PyMol software.

Fig. 6 **Reactivity profiles of furin variable loop mutants with synthetic substrate and serpin inhibitors** Bar graphs depicting the effects of mutating the four variable surface loops of furin to alanines on k_{cat}/K_M for furin cleavage of a tetrapeptide fluorogenic substrate and on k_{ass} for furin reactions with serpin B8-5S, α_1PDX, and α_1PDX-serpin B8 P6-P1, P1'-P5' and P6-P5' chimeras. k_{cat}/K_M values are taken from table 2 and k_{ass} values are from table 3. Numbers at the top of bars represent kinetic constants expressed relative to wild-type furin values.

Fig. 7 **Reactivity profiles of furin 298-300 loop PC chimeras with synthetic substrate and serpin inhibitors.** Bar graphs showing the effects of substituting the 298-300 loop of furin with the corresponding loop sequences of other PC family members on k_{cat}/K_M for furin reaction with a tetrapeptide fluorogenic substrate, and on k_{ass} for furin reactions with serpin B8-5S5A, with α_1PDX, and with the α_1PDX-serpin B8 P6-P5' chimera. Values of k_{cat}/K_M are taken from table 4 and values of k_{ass} are from table 5. Values at the top of bars are kinetic constants expressed relative to the value for wild-type furin.

Fig. 8 **Molecular model of the serpin B8-furin Michaelis complex** The complex is depicted as ribbon structures with serpin B8 in yellow and the furin catalytic domain in white. Highlighted in stick are the furin 298-300 loop residues (green), serpin B8 residues Phe198 and Glu200 of strand 3 of β-sheet C (red) and the serpin B8 P1 residue (red). The complex shown was modeled based on the antithrombin-S195A factor Xa Michaelis complex structure but modeling based on two other Michaelis complex structures gave similar results (see Experimental Procedures). The proximity of the furin loop and the strand 3C exosite residues is evident. The figure was prepared using PyMol software.

Fig. 9 **Reactivity profiles of α_1PDX exosite variants with furin loop variants** Reactivity of α_1PDX-YE exosite variant with furin variable loop mutants and with furin 298-300 loop chimeras (left-hand panels). Reactivity of α_1PDX-serpin B8 P6-P5'-YE dual chimera with the furin variable loop mutants and 298-300 loop chimeras (right-hand panels). k_{ass} values are from tables 3 and 5. Reactivity profiles of the furin loop variants with α_1PDX variants are expressed relative to wild-type furin reactivities.

Fig. 10 **Coupling effects of RCL and strand 3C substitutions on α_1PDX reactivity with furin** A, Double mutation cycle for substitution of serpin B8 RCL and strand 3C sequences into α_1PDX. Small letters indicate the relative change in k_{ass} resulting from the mutations indicated by the arrow. B, Fold changes in k_{ass} for reactions of α_1PDX with furin and the indicated furin loop variants resulting from individual or combined RCL and s3C substitutions in α_1PDX. The coupling index indicates the ratio of the relative changes in k_{ass} for one set of mutations in the presence or absence of the second set of mutations. A value of 1 indicates no coupling.

TABLES

Table 1. **Kinetic constants and stoichiometries of inhibition for reactions of furin with wild-type and variant forms of serpin B8 and α_1PDX** Association rate constants (k_{ass}) and stoichiometries of inhibition (SI) for serpin-furin reactions were measured at pH 7.5, 25°C, as described in the legend to fig. 1 and in Experimental Procedures. Errors represent standard errors (S.E.) from linear regression fits of data. The SI for the serpin B8 R342A mutant was assumed to be 1 based on the absence of detectable cleaved serpin product in the reaction by SDS-PAGE analysis (fig. 2).

Inhibitor Variant	k_{ass} ($M^{-1} s^{-1}$)	SI
Serpin B8 - 5S	2.4 ± 0.3 x 10^5	1.5 ± 0.1
Serpin B8 - 5S5A	2.3 ± 0.2 x 10^5	2.2 ± 0.1
Serpin B8 - 5S- R342A	7.6 ± 0.5 x 10^4	1
α_1PDX	1.1 ± 0.1 x 10^6	1.1 ± 0.1
α_1PDX - Serpin B8 P6-P1	2.5 ± 0.3 x 10^6	1.3 ± 0.1
α_1PDX - Serpin B8 P1'-P5'	5.5 ± 0.8 x 10^4	1.2 ± 0.1
α_1PDX - Serpin B8 P6-P5'	1.1 ± 0.1 x 10^5	1.4 ± 0.1
α_1PDX - YE	2.1 ± 0.3 x 10^5	1.9 ± 0.1
α_1PDX - Serpin B8 P6-P5' - YE	1.5 ± 0.2 x 10^3	1.3 ± 0.2

Table 2. **Kinetic constants for the catalytic reaction of furin and furin alanine loop mutants with two RXXR fluorogenic substrates.** Kinetic constants were measured at pH 7.5, 25°C from the dependence of initial rates of substrate hydrolysis on substrate concentration as described in Experimental Procedures. Errors represent standard errors (S.E.) from nonlinear regression fits of data by the Michaelis-Menten equation.

Furin Surface Loop Variant	Furin Residues Mutated into Alanines	boc - R V R R - amc				pyr - R T K R - amc			
		K_M (μM)	k_{cat} (s^{-1})	k_{cat}/K_M ($M^{-1}s^{-1}$)	k_{cat}/K_M Variant / wt Ratio	K_M (μM)	k_{cat} (s^{-1})	k_{cat}/K_M ($M^{-1}s^{-1}$)	k_{cat}/K_M Variant / wt Ratio
Wild-type	---	28.2 ± 1.3	0.27 ± 0.01	9.2 ± 1.0 x 10^3	1	4.7 ± 0.5	0.16 ± 0.00	3.4 ± 0.7 x 10^4	1
187-189	TQM	25.1 ± 2.7	0.03 ± 0.00	1.1 ± 0.2 x 10^3	0.12 ± 0.03	9.0 ± 1.0	0.05 ± 0.00	6.1 ± 1.1 x 10^3	0.18 ± 0.07
298-300	REH	20.2 ± 1.2	0.09 ± 0.01	4.5 ± 0.7 x 10^3	0.49 ± 0.13	5.0 ± 0.4	0.10 ± 0.00	2.1 ± 0.3 x 10^4	0.62 ± 0.21
345-350	NQNEKQ	23.3 ± 1.9	0.19 ± 0.03	8.1 ± 1.6 x 10^3	0.88 ± 0.27	5.4 ± 0.3	0.15 ± 0.03	2.7 ± 0.6 x 10^4	0.73 ± 0.31
357-359	RQK	8.7 ± 0.7	0.03 ± 0.00	2.9 ± 0.3 x 10^3	0.32 ± 0.07	5.8 ± 0.6	0.08 ± 0.01	1.3 ± 0.2 x 10^4	0.38 ± 0.14

Table 3. **Kinetic constants and stoichiometries of inhibition for the reactions of serpin B8, α_1PDX, and α_1PDX-serpin B8 chimeras with furin and furin alanine loop mutants.** Values of k_{ass} and SI ±S.E. for serpin-furin reactions were measured at pH 7.5, 25°C as in table 1. SIs for the reactions of α_1PDX-serpin B8 P6-P5'-YE chimera with the furin loop mutants could not be determined (ND) because of enzyme instability over the long times required for complete reaction.

Furin Surface Loop Variant	Serpin B8		α_1PDX		α_1PDX-Serpin B8 P6-P1		α_1PDX-Serpin B8 P1'-P5'		α_1PDX-Serpin B8 P6-P5'		α_1PDX-YE		α_1PDX-Serpin B8 P6-P5'-YE	
	k_{ass} ($M^{-1}s^{-1}$)	SI	k_{ass} ($M^{-1}s^{-1}$)	SI	k_{ass} ($M^{-1}s^{-1}$)	SI	k_{ass} ($M^{-1}s^{-1}$)	SI	k_{ass} ($M^{-1}s^{-1}$)	SI	k_{ass} ($M^{-1}s^{-1}$)	SI	k_{ass} ($M^{-1}s^{-1}$)	SI
Wild-type	$2.4 \pm 0.3 \times 10^5$	1.5 ± 0.1	$1.1 \pm 0.1 \times 10^6$	1.1 ± 0.1	$2.5 \pm 0.3 \times 10^6$	1.3 ± 0.1	$5.5 \pm 0.8 \times 10^4$	1.2 ± 0.1	$1.1 \pm 0.1 \times 10^5$	1.4 ± 0.1	$2.1 \pm 0.3 \times 10^5$	1.9 ± 0.1	$1.5 \pm 0.2 \times 10^3$	1.3 ± 0.2
187-189	$5.6 \pm 0.9 \times 10^4$	1.2 ± 0.2	$3.8 \pm 0.8 \times 10^5$	0.9 ± 0.1	$3.5 \pm 0.3 \times 10^5$	1.3 ± 0.1	$2.0 \pm 0.3 \times 10^4$	1.0 ± 0.0	$2.5 \pm 1.0 \times 10^4$	1.5 ± 0.1	$4.2 \pm 0.7 \times 10^4$	1.0 ± 0.1	$5.5 \pm 0.4 \times 10^2$	ND
298-300	$6.1 \pm 1.3 \times 10^4$	1.5 ± 0.3	$1.8 \pm 0.1 \times 10^6$	1.2 ± 0.1	$2.7 \pm 0.3 \times 10^6$	1.4 ± 0.0	$2.3 \pm 0.2 \times 10^4$	1.0 ± 0.0	$1.9 \pm 0.9 \times 10^4$	1.0 ± 0.1	$1.3 \pm 0.1 \times 10^5$	0.8 ± 0.2	$1.5 \pm 0.1 \times 10^3$	ND
345-350	$1.5 \pm 0.2 \times 10^5$	1.1 ± 0.1	$5.2 \pm 0.5 \times 10^5$	1	$6.7 \pm 0.9 \times 10^5$	1.0 ± 0.1	$4.7 \pm 1.1 \times 10^4$	1.1 ± 0.2	$8.9 \pm 1.7 \times 10^4$	1.8 ± 0.1	$1.7 \pm 0.3 \times 10^5$	1.3 ± 0.1	$1.4 \pm 0.0 \times 10^3$	ND
357-359	$5.6 \pm 1.1 \times 10^4$	1.3 ± 0.2	$7.1 \pm 1.0 \times 10^5$	0.8 ± 0.1	$8.5 \pm 0.9 \times 10^5$	1.0 ± 0.0	$5.2 \pm 1.1 \times 10^4$	0.9 ± 0.1	$7.4 \pm 1.9 \times 10^4$	1.3 ± 0.1	$6.9 \pm 1.0 \times 10^4$	0.8 ± 0.2	$1.0 \pm 0.2 \times 10^3$	ND

Table 4. **Kinetic constants for the catalytic reaction of furin-PC 298-300 loop chimeras with RXXR fluorogenic substrate.** Kinetic parameters were determined at pH 7.5, 25°C as in table 2.

Furin-PC Chimeras	Amino Acid Sequence at Loop 298-300	boc - R V R R - amc			
		K_M (μM)	k_{cat} (s^{-1})	k_{cat}/K_M ($M^{-1}s^{-1}$)	k_{cat}/K_M Variant / wt Ratio
Wild-type	R E H	28.2 ± 1.3	0.27 ± 0.01	9.2 ± 1.0 x 10^3	1
F-PC1	R Q G	27.6 ± 2.3	0.17 ± 0.01	6.2 ± 1.0 x 10^3	0.67 ± 0.18
F-PC2	S Y -	20.0 ± 1.5	0.09 ± 0.01	4.6 ± 0.8 x 10^3	0.50 ± 0.14
F-PC4	L H Y	34.3 ± 2.4	0.24 ± 0.03	7.0 ± 1.3 x 10^3	0.76 ± 0.22
F-PC5/6	R S K	45.7 ± 2.7	0.13 ± 0.02	2.8 ± 0.5 x 10^3	0.30 ± 0.09
F-PACE4	R E G	27.0 ± 1.5	0.27 ± 0.01	9.7 ± 1.0 x 10^3	1.1 ± 0.23
F-PC7	Q H N	23.9 ± 1.8	0.29 ± 0.06	1.2 ± 0.3 x 10^4	1.3 ± 0.47
298-300	AAA	20.5 ± 2.9	0.09 ± 0.01	4.4 ± 0.8 x 10^3	0.48 ± 0.14

Table 5. **Kinetic constants and stoichiometries of inhibition for reactions of serpin B8, α_1PDX, and α_1PDX-serpin B8 chimeras with furin and furin-PC 298-300 loop chimeras.** Values of k_{ass} and SI ±S.E. for serpin-furin reactions were measured at pH 7.5, 25°C as in table 1. SIs for the reactions of α_1PDX-serpin B8 P6-P5'-YE chimera with the furin-PC loop chimeras could not be determined (ND) because of enzyme instability over the long times required for complete reaction.

Furin-PC Chimeras	Serpin B8		α_1PDX		α_1PDX-Serpin B8 P6-P5'		α_1PDX-YE		α_1PDX-Serpin B8 P6-P5'-YE	
	k_{ass} ($M^{-1} s^{-1}$)	SI	k_{ass} ($M^{-1} s^{-1}$)	SI	k_{ass} ($M^{-1} s^{-1}$)	SI	k_{ass} ($M^{-1} s^{-1}$)	SI	k_{ass} ($M^{-1} s^{-1}$)	SI
Wild-type	2.3 ± 0.2 x 10^5	2.2 ± 0.1	1.1 ± 0.1 x 10^6	1.1 ± 0.1	1.1 ± 0.1 x 10^5	1.4 ± 0.1	2.1 ± 0.7 x 10^5	1.9 ± 0.1	1.5 ± 0.2 x 10^3	1.3 ± 0.2
F-PC1	9.8 ± 1.2 x 10^4	1.4 ± 0.1	2.6 ± 0.5 x 10^6	1.7 ± 0.2	7.1 ± 1.4 x 10^4	1.3 ± 0.1	9.3 ± 1.7 x 10^5	1.3 ± 0.1	5.6 ± 0.1 x 10^3	ND
F-PC2	6.4 ± 1.4 x 10^4	1.6 ± 0.2	1.1 ± 0.2 x 10^6	1.5 ± 0.1	5.3 ± 0.5 x 10^4	0.9 ± 0.1	1.7 ± 0.2 x 10^5	1.2 ± 0.1	9.2 ± 0.7 x 10^2	ND
F-PC4	1.3 ± 0.1 x 10^5	1.6 ± 0.1	1.0 ± 0.2 x 10^6	1.4 ± 0.2	6.4 ± 0.9 x 10^4	1.6 ± 0.1	2.4 ± 0.5 x 10^5	1.3 ± 0.2	3.4 ± 0.2 x 10^3	ND
F-PC5/6	4.9 ± 0.6 x 10^4	1.1 ± 0.1	2.2 ± 0.4 x 10^6	1.5 ± 0.2	6.4 ± 1.5 x 10^4	0.9 ± 0.1	9.4 ± 1.6 x 10^5	1.2 ± 0.2	2.6 ± 0.3 x 10^4	ND
F-PACE4	9.4 ± 0.9 x 10^4	1.8 ± 0.1	1.6 ± 0.3 x 10^6	1.9 ± 0.3	1.3 ± 0.1 x 10^5	0.8 ± 0.2	2.4 ± 0.5 x 10^5	1.4 ± 0.3	1.0 ± 0.1 x 10^3	ND
F-PC7	2.5 ± 0.4 x 10^5	2.1 ± 0.1	1.0 ± 0.2 x 10^6	1.4 ± 0.1	6.0 ± 0.7 x 10^4	1.3 ± 0.1	2.4 ± 0.2 x 10^5	1.1 ± 0.0	3.0 ± 0.1 x 10^3	ND
298-300 AAA	6.1 ± 1.3 x 10^4	1.5 ± 0.3	1.8 ± 0.1 x 10^6	1.2 ± 0.1	1.9 ± 0.8 x 10^4	1.0 ± 0.1	1.3 ± 0.1 x 10^5	0.8 ± 0.2	1.5 ± 0.1 x 10^3	ND

Figure 1

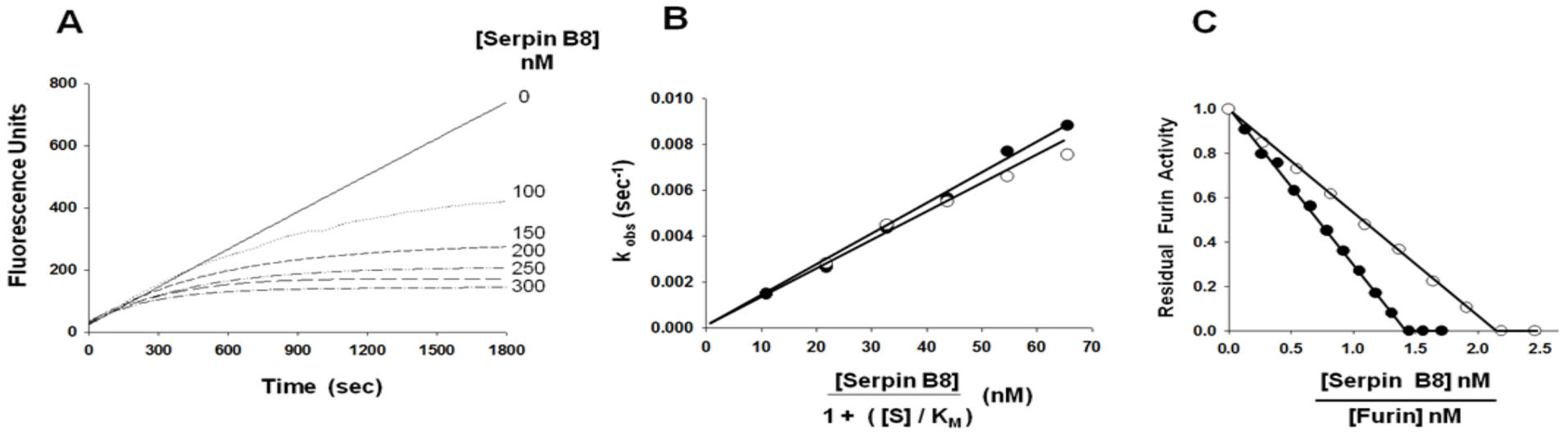

Figure 2

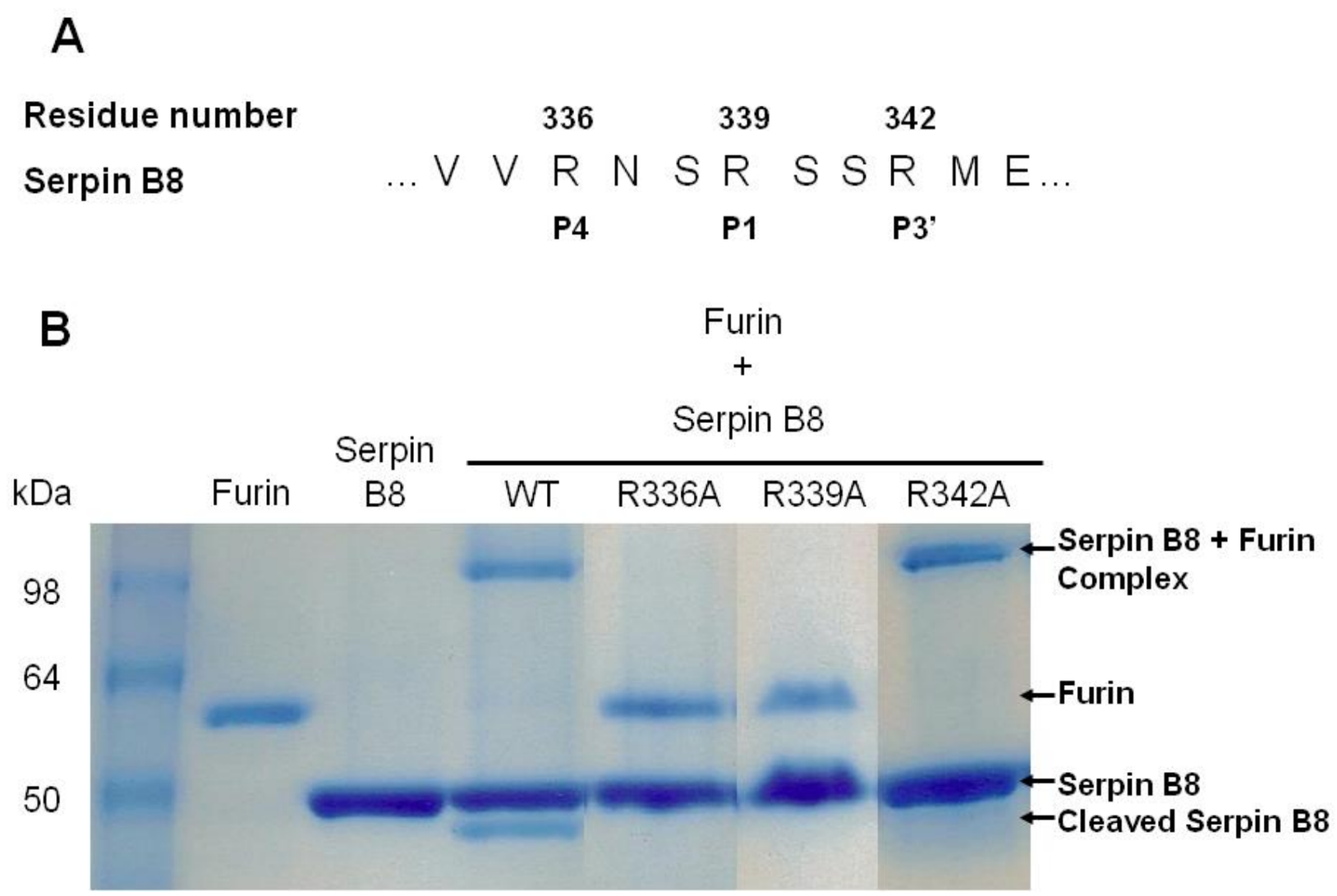
A
Residue number
336
339
342
Serpin B8
... V V R N S R S S R M E ...
P4
P1
P3'
B
Furin
+
Serpin B8
kDa
Furin
Serpin B8
WT
R336A
R339A
R342A
98
64
50
Serpin B8 + Furin Complex
Furin
Serpin B8
Cleaved Serpin B8

Figure 3

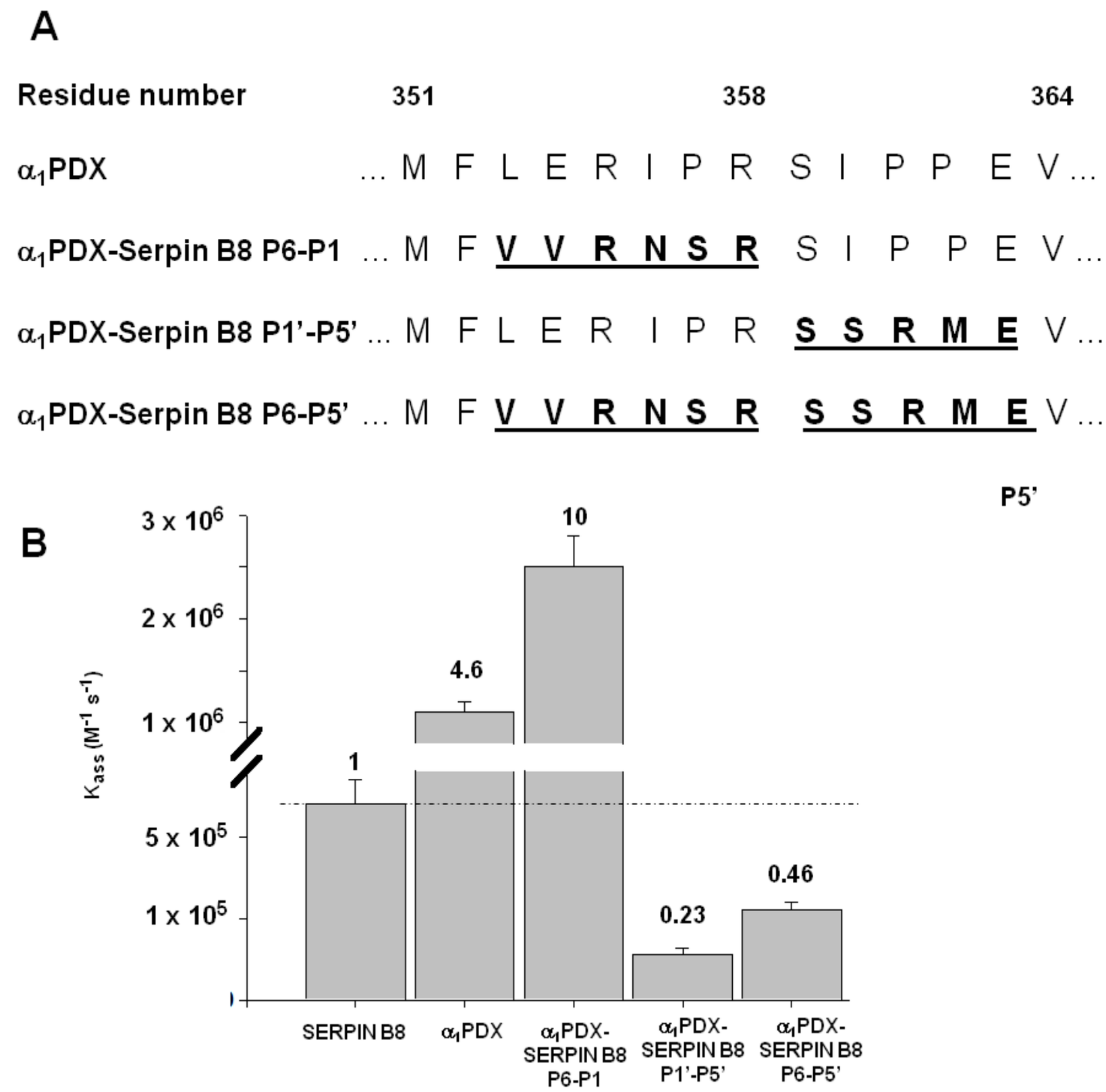

Figure 4

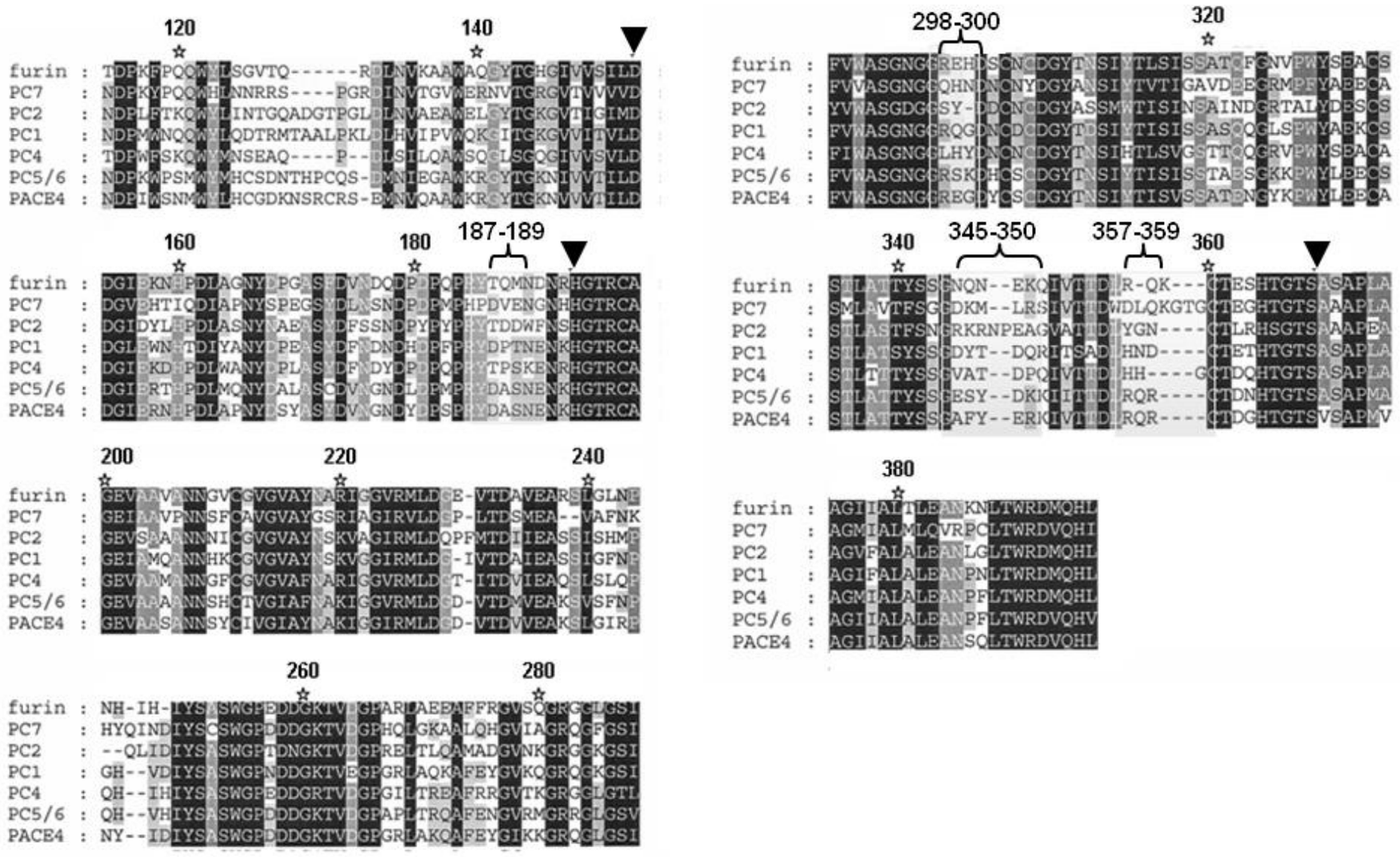

Figure 5

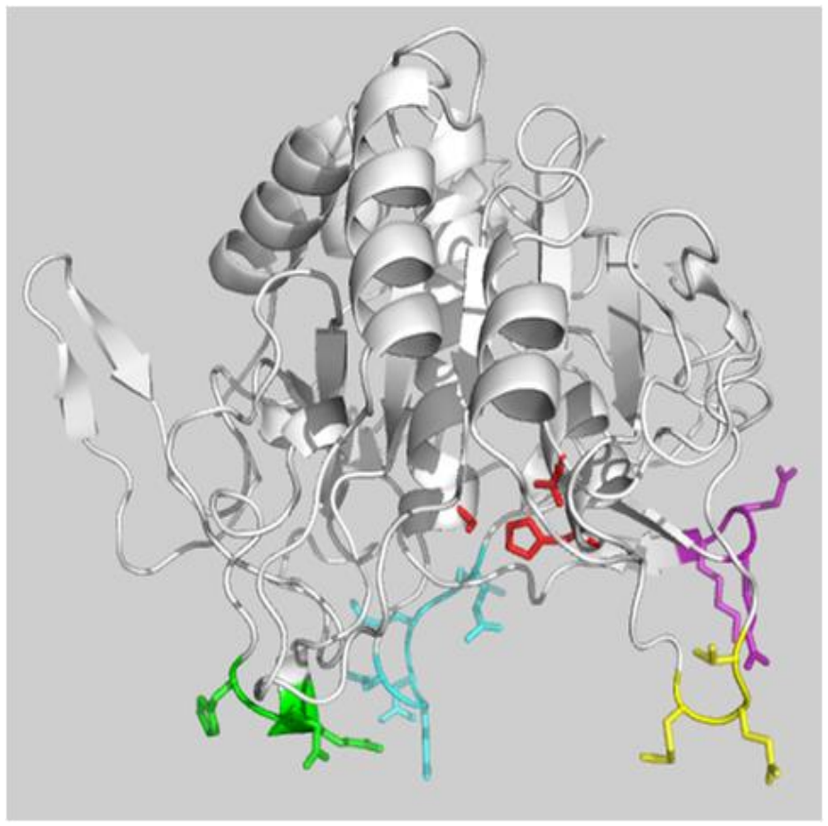

Figure 6

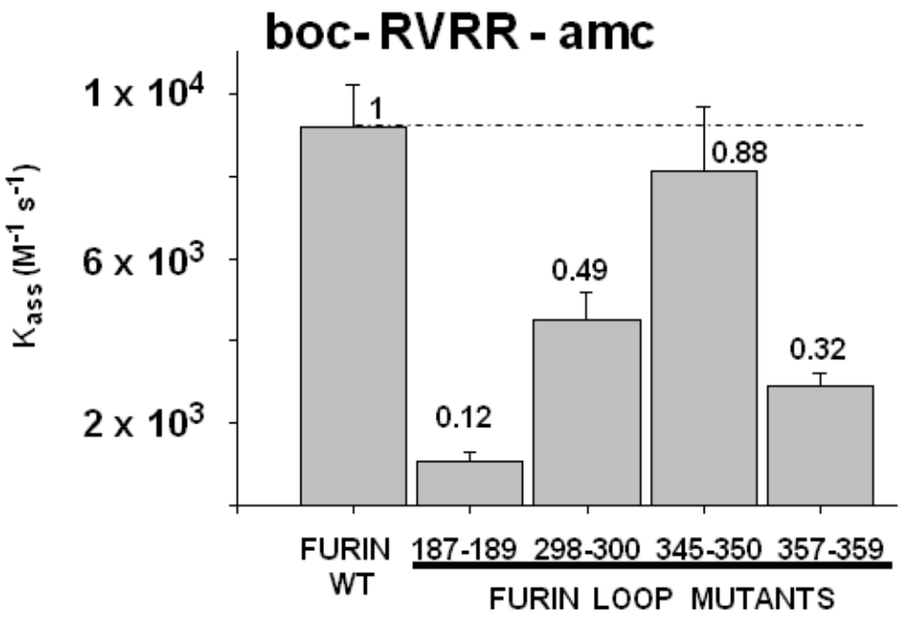
boc- RVRR - amc
K_{ass} (M^{-1} s^{-1})
1 x 10^4
6 x 10^3
2 x 10^3
1
0.12
0.49
0.88
0.32
FURIN WT
187-189 298-300 345-350 357-359
FURIN LOOP MUTANTS

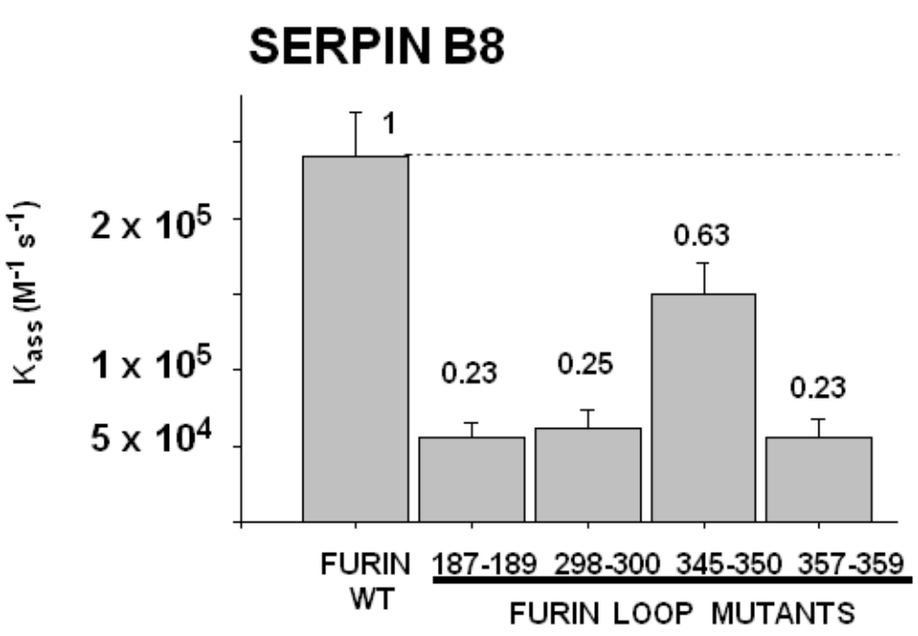
SERPIN B8
K_{ass} (M^{-1} s^{-1})
2 x 10^5
1 x 10^5
5 x 10^4
1
0.23
0.25
0.63
0.23
FURIN WT
187-189 298-300 345-350 357-359
FURIN LOOP MUTANTS

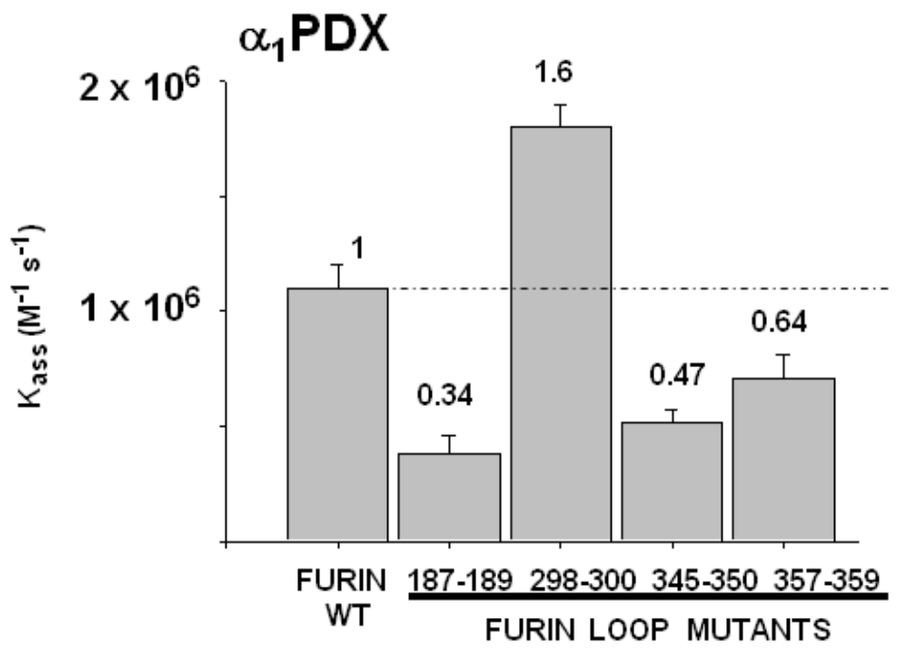
α_1PDX
K_{ass} (M^{-1} s^{-1})
2 x 10^6
1 x 10^6
1
0.34
1.6
0.47
0.64
FURIN WT
187-189 298-300 345-350 357-359
FURIN LOOP MUTANTS

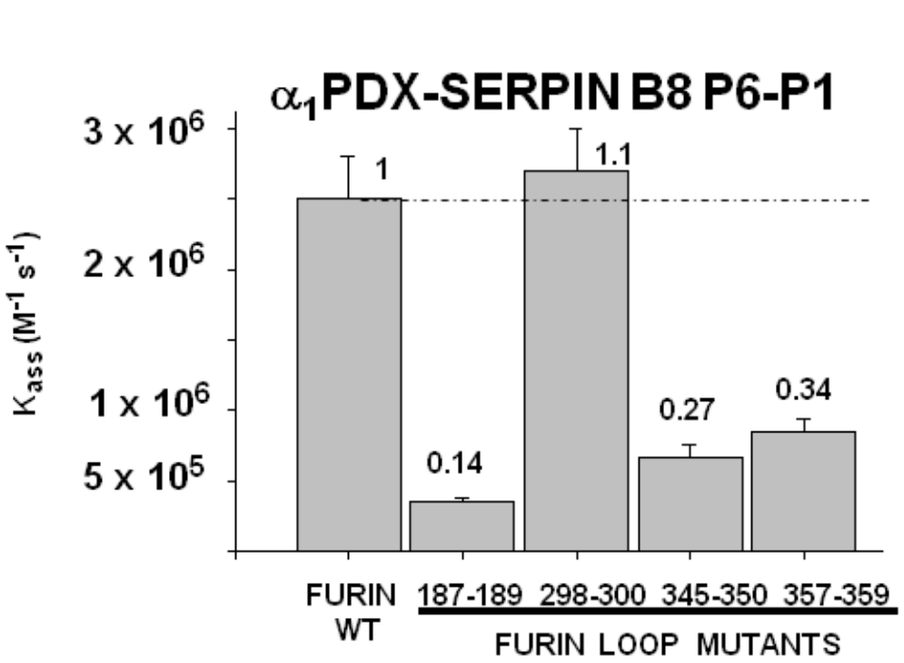
α_1PDX-SERPIN B8 P6-P1
K_{ass} (M^{-1} s^{-1})
3 x 10^6
2 x 10^6
1 x 10^6
5 x 10^5
1
0.14
1.1
0.27
0.34
FURIN WT
187-189 298-300 345-350 357-359
FURIN LOOP MUTANTS

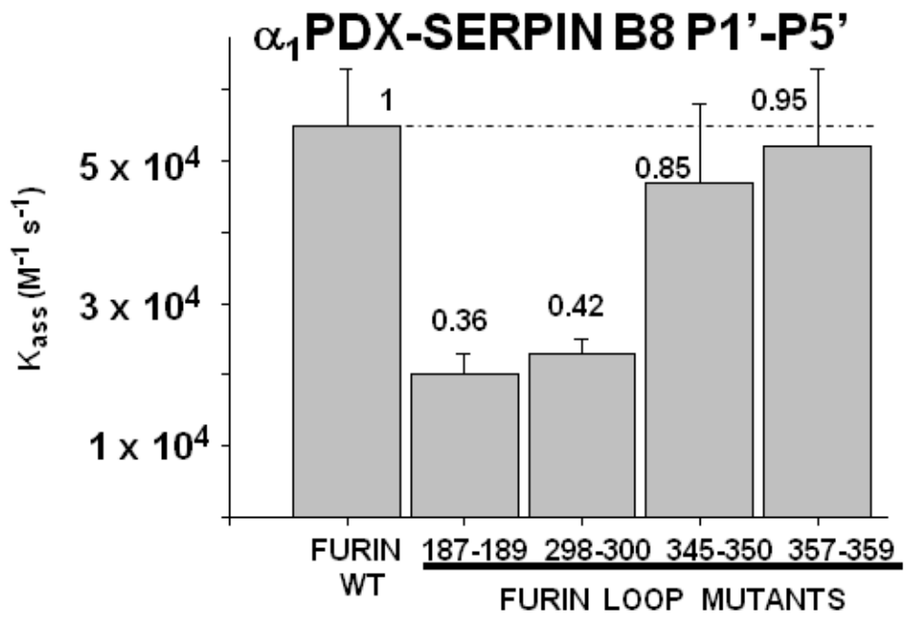
α_1PDX-SERPIN B8 P1'-P5'
K_{ass} (M^{-1} s^{-1})
5 x 10^4
3 x 10^4
1 x 10^4
1
0.36
0.42
0.85
0.95
FURIN WT
187-189 298-300 345-350 357-359
FURIN LOOP MUTANTS

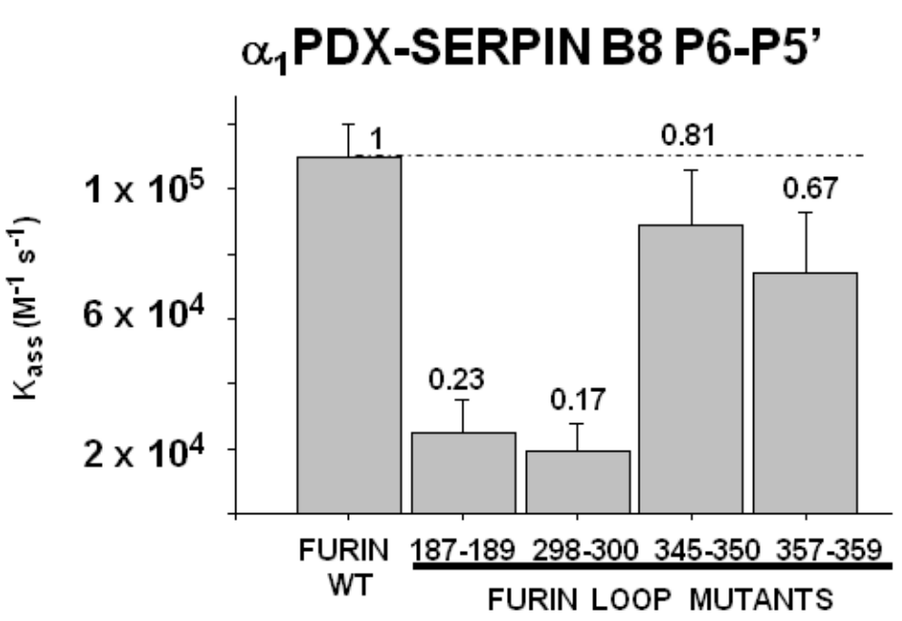
α_1PDX-SERPIN B8 P6-P5'
K_{ass} (M^{-1} s^{-1})
1 x 10^5
6 x 10^4
2 x 10^4
1
0.23
0.17
0.81
0.67
FURIN WT
187-189 298-300 345-350 357-359
FURIN LOOP MUTANTS

Figure 7

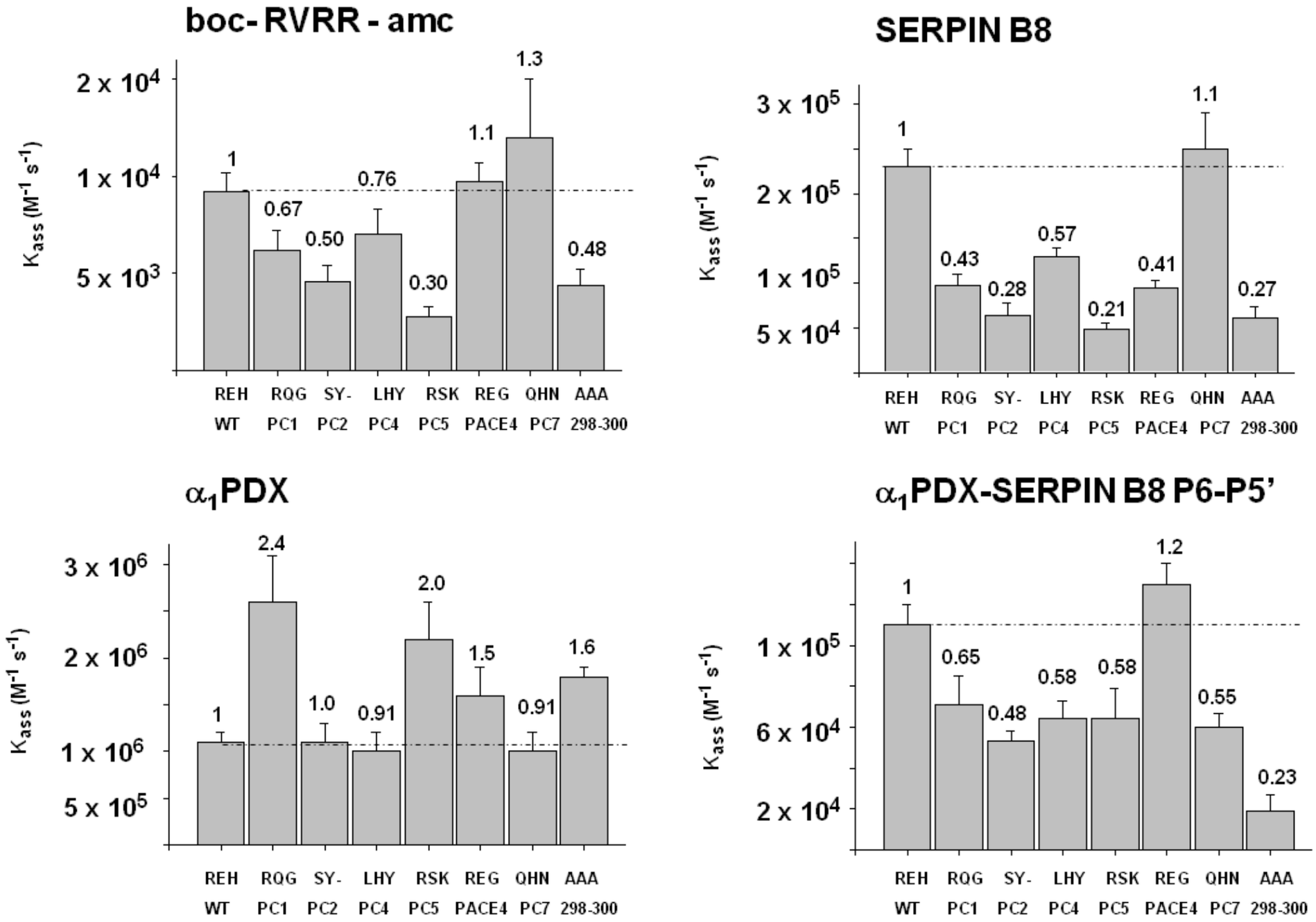

Figure 8

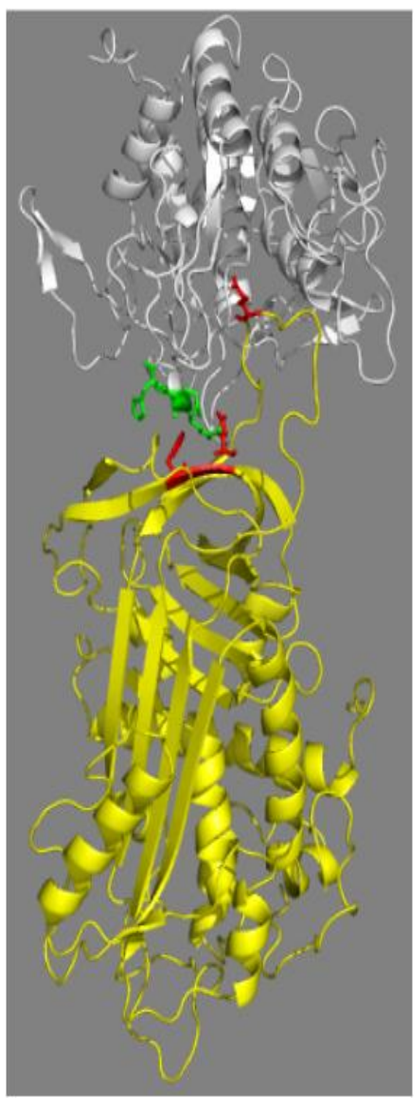

Figure 9

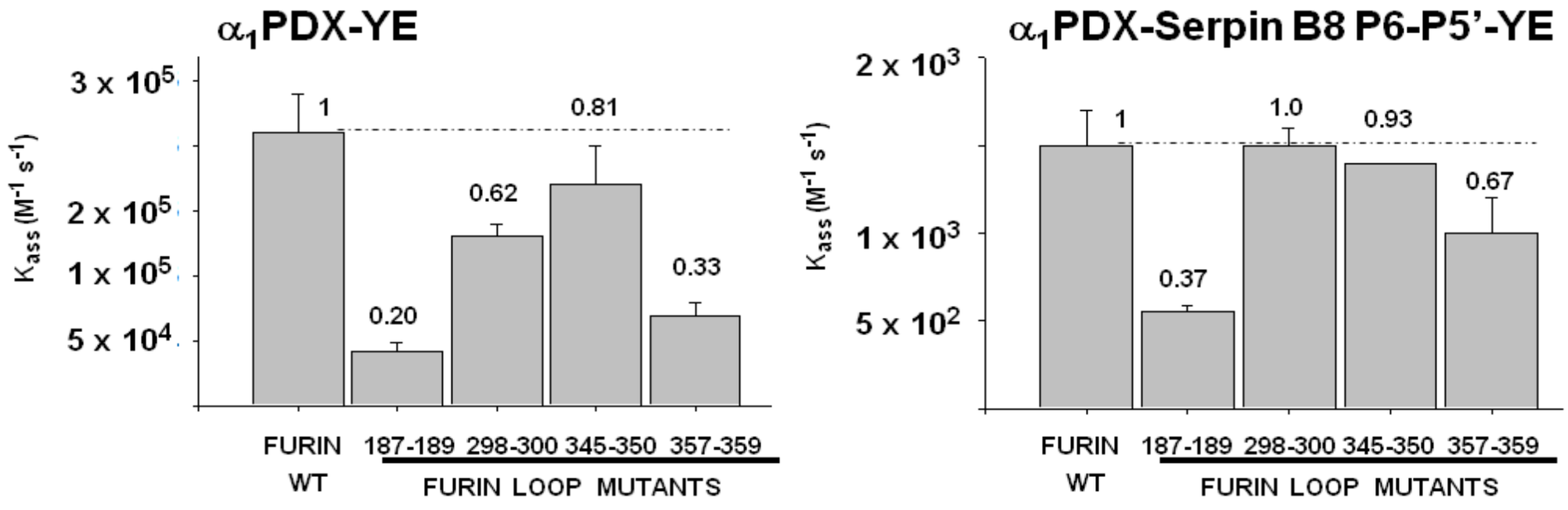
α1PDX-YE
Kass (M-1 s-1)
3 x 10^5
2 x 10^5
1 x 10^5
5 x 10^4
1
0.20
0.62
0.81
0.33
FURIN WT
187-189 298-300 345-350 357-359
FURIN LOOP MUTANTS
α1PDX-Serpin B8 P6-P5'-YE
Kass (M-1 s-1)
2 x 10^3
1 x 10^3
5 x 10^2
1
0.37
1.0
0.93
0.67
FURIN WT
187-189 298-300 345-350 357-359
FURIN LOOP MUTANTS
α1PDX-YE
Kass (M-1 s-1)
1 x 10^6
6 x 10^5
2 x 10^5
1
4.4
0.81
1.1
4.5
1.1
1.1
0.62
REH WT
RQG PC1
SY- PC2
LHY PC4
RSK PC5
REG PACE4
QHN PC7
AAA 298-300
α1PDX-Serpin B8 P6-P5'-YE
Kass (M-1 s-1)
3 x 10^4
2 x 10^4
6 x 10^3
3 x 10^3
1
3.7
0.62
2.3
17
0.67
2.0
1.0
REH WT
RQG PC1
SY- PC2
LHY PC4
RSK PC5
REG PACE4
QHN PC7
AAA 298-300

Figure 10

A

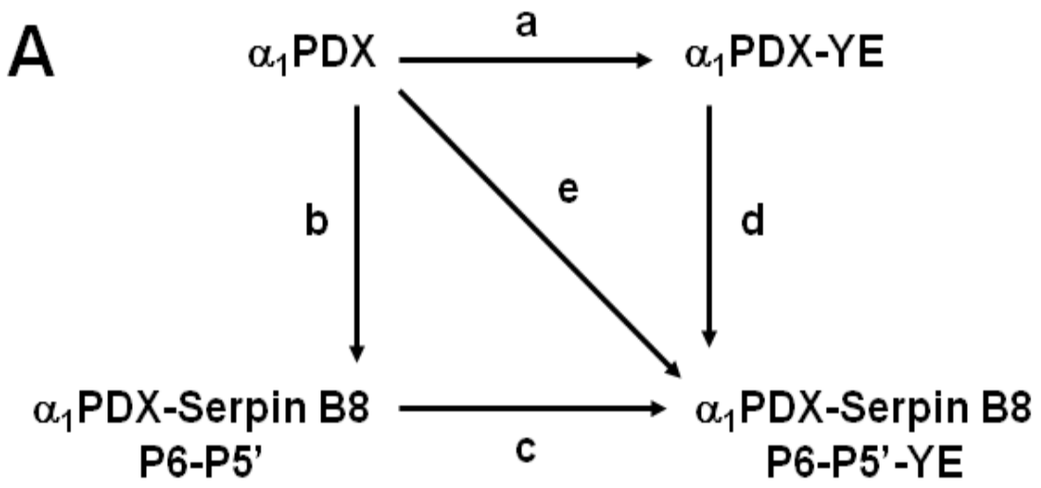

B

Furin Variant	Fold Change is k_{ass}					Coupling Index
	a	b	c	d	e	c / a = d / b
Wild-type	5.2	10	73	140	733	14
187-189	9	15	45	76	691	5.0
298-300	12	95	13	89	1200	1.0
345-350	3.1	5.8	64	121	371	21
357-359	10	9.6	74	69	710	7.3
F-PC1	2.8	37	13	166	464	4.6
F-PC2	6.5	21	58	185	1196	8.9
F-PC4	4.2	16	19	71	294	4.5
F-PC5/6	2.3	34	2.5	36	85	1.1
F-PACE4	6.7	12	130	240	1600	19
F-PC7	4.2	17	20	80	333	4.8